JACS
JOURNAL OF THE AMERICAN CHEMICAL SOCIETY

Subscriber access provided by American Chemical Society

Article

Carbon–Fluorine Bond Activation Coupled with Carbon–Carbon Bond Formation at Iridium. Confirmation of Complete Kinetic Diastereoselectivity at the New Carbon Stereocenter by Intramolecular Trapping Using Vinyl as the Migrating Group

Russell P. Hughes, Roman B. Laritchev, Lev N. Zakharov, and Arnold L. Rheingold

J. Am. Chem. Soc., **2005**, 127 (17), 6325-6334• DOI: 10.1021/ja042345d • Publication Date (Web): 05 April 2005

Downloaded from http://pubs.acs.org on March 25, 2009

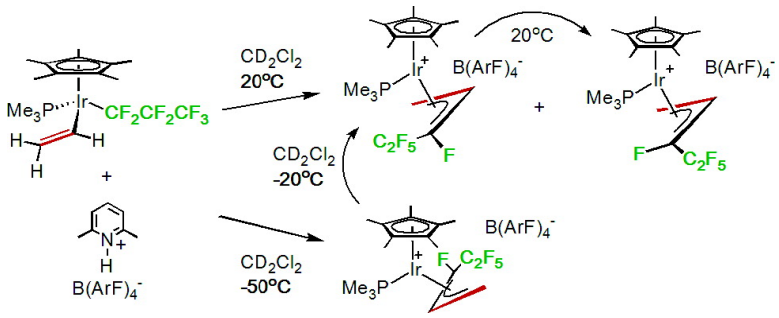

More About This Article

Additional resources and features associated with this article are available within the HTML version:

- Supporting Information
- Links to the 6 articles that cite this article, as of the time of this article download
- Access to high resolution figures
- Links to articles and content related to this article
- Copyright permission to reproduce figures and/or text from this article

View the Full Text HTML

ACS Publications
High quality. High impact.

Journal of the American Chemical Society is published by the American Chemical Society. 1155 Sixteenth Street N.W., Washington, DC 20036

J|A|C|S
ARTICLES
Published on Web 04/05/2005

Carbon−Fluorine Bond Activation Coupled with Carbon−Carbon Bond Formation at Iridium. Confirmation of Complete Kinetic Diastereoselectivity at the New Carbon Stereocenter by Intramolecular Trapping Using Vinyl as the Migrating Group

Russell P. Hughes,*,† Roman B. Laritchev,† Lev N. Zakharov,‡ and Arnold L. Rheingold‡

Contribution from the Departments of Chemistry, 6128 Burke Laboratory, Dartmouth College, Hanover, New Hampshire 03755, and University of California, San Diego, California 92093-0358

Received December 20, 2004; E-mail: rph@dartmouth.edu

Abstract: The iridium(perfluoropropyl)(vinyl) complex Cp*Ir(PMe_3)(*n*-C_3F_7)(CH═CH_2) (**5**) has been prepared. It has been characterized by X-ray crystallography, and its ground state conformation in solution has been determined by $^{19}F\{^1H\}$ HOESY NMR studies. It reacts with the weak acid lutidinium iodide to afford the η^1-allylic complex Cp*Ir(PMe_3)((Z)-CH_2CH═CFC_2F_5)I (**6**), which has also been characterized crystallographically. The mechanism of C−F bond activation and C−C bond formation leading to **6** has been elucidated in detail by studying the reaction of **5** with lutidinium tetrakis[3,5-bis(trifluoromethyl)phenyl]borate [$LutH^+B(ArF)_4^-$], containing a weakly coordinating counteranion. The main kinetic product of this reaction, determined by $^{19}F\{^1H\}$ HOESY studies at −50 °C, is the *endo*-Cp*Ir(PMe_3)(*anti*-η^3-$CH_2CHCFCF_2CF_3$)-[$B(ArF)_4$] diastereomer **9**, along with a small amount of the *exo-syn*-isomer **8**. Isomer **9** rearranges at −20 °C to its *exo-anti* isomer **7**, and subsequently to the thermodynamically favored *exo-syn*-isomer **8**, which has been isolated and crystallographically characterized. Complex **8** reacts with iodide to afford complex **6**. On the basis of the unambiguously defined kinetically controlled stereochemistry of **9** and **8**, a detailed mechanism for the C−F activation/C−C coupling reaction is proposed, the principal conclusion of which is that C−F activation is completely diastereoselective.

Introduction

The activation of aliphatic carbon−fluorine bonds using transition metal complexes has been a topic of long-standing interest. A variety of methods, including strongly reducing conditions[1−9] and radical-based transition metal chemistry,[10−13] have been employed. The roots of this interest are many, including perhaps most prominently the conversion of environmentally harmful chlorofluorocarbons (CFCs) and perfluorocarbons (PFCs) to more friendly and useful fluorocarbon compounds,[14,15] coupled with the intellectual challenge of activating the strongest single bond to carbon[16] in molecules originally designed to be chemically inert.[17]

Almost all successful attempts to generate fluorinated stereocenters in organic molecules rely on C−F bond formation approaches, in some cases with the assistance of transition metal complexes.[18−29] The asymmetric synthesis of carbon stereo-

† Dartmouth College.
‡ University of California, San Diego.

(1) Richmond, T. G. *Top. Organomet. Chem.* **1999**, *3*, 243−269.
(2) McAlexander, L. H.; Beck, C. M.; Burdeniuc, J. J.; Crabtree, R. H. *J. Fluor. Chem.* **1999**, *99*, 67−72.
(3) Burdeniuc, J.; Siegbahn, P. E. M.; Crabtree, R. H. *New J. Chem.* **1998**, *22*, 503−510.
(4) Burdeniuc, J.; Jedlicka, B.; Crabtree, R. H. *Chem. Ber./Recl.* **1997**, *130*, 145−154.
(5) Kiplinger, J. L.; Richmond, T. G. *J. Am. Chem. Soc.* **1996**, *118*, 1805−1806.
(6) Bennett, B. K.; Harrison, R. G.; Richmond, T. G. *J. Am. Chem. Soc.* **1994**, *116*, 11165−11166.
(7) Harrison, R. G.; Richmond, T. G. *J. Am. Chem. Soc.* **1993**, *115*, 5303−5304.
(8) Kiplinger, J. L.; Richmond, T. G. *Chem. Commun.* **1996**, 1115−1116.
(9) Hughes, R. P.; Laritchev, R. B.; Zakharov, L. N.; Rheingold, A. L. *J. Am. Chem. Soc.* **2004**, *126*, 2308−2309.
(10) Jones, W. D. *Dalton Trans.* **2003**, 3991−3995.
(11) Kraft, B. M.; Lachicotte, R. J.; Jones, W. D. *J. Am. Chem. Soc.* **2000**, *122*, 8559−8560.
(12) Kraft, B. M.; Lachicotte, R. J.; Jones, W. D. *J. Am. Chem. Soc.* **2001**, *123*, 10973−10979.
(13) Clot, E.; Mégret, C.; Kraft, B. M.; Eisenstein, O.; Jones, W. D. *J. Am. Chem. Soc.* **2004**, *126*, 5647−5653.
(14) Manzer, L. E. *Chem. Ind.* **1994**, *53*, 411−418.
(15) Manzer, L. E. *Science* **1990**, *249*, 31−35.
(16) Smart, B. E. Fluorocarbons. In *Chemistry of Functional Groups, Supplement D*; Patai, S., Rappoport, Z., Eds.; Wiley, New York: 1983; Chapter 14, pp 603−655.
(17) Lemal, D. M. *J. Org. Chem.* **2004**, *69*, 1−11.
(18) Baudequin, C.; Loubassou, J.-F.; Plaquevent, J.-C.; Cahard, D. *J. Fluor. Chem.* **2002**, *122*, 189−193.
(19) Ma, J.-A.; Cahard, D. *Chem. Rev.* **2004**, *104*, 6119−6146.
(20) Gouverneur, V.; Greedy, B. *Chem. Eur. J.* **2002**, *8*, 766−771.
(21) Mohar, B.; Baudoux, J.; Plaquevent, J.-C.; Cahard, D. *Angew. Chem., Int. Ed.* **2001**, *40*, 4214−4216.
(22) Piana, S.; Devillers, I.; Togni, A.; Rothlisberger, U. *Angew. Chem., Int. Ed.* **2002**, *41*, 979−982.
(23) Prakesch, M.; Grée, D.; Grée, R. *Acc. Chem. Res.* **2002**, *35*, 175−181.
(24) Muniz, K. *Angew. Chem., Int. Ed.* **2001**, *40*, 1653−1656.
(25) Shibata, N.; Suzuki, E.; Asahi, T.; Shiro, M. *J. Am. Chem. Soc.* **2001**, *123*, 7001−7009.

Scheme 1

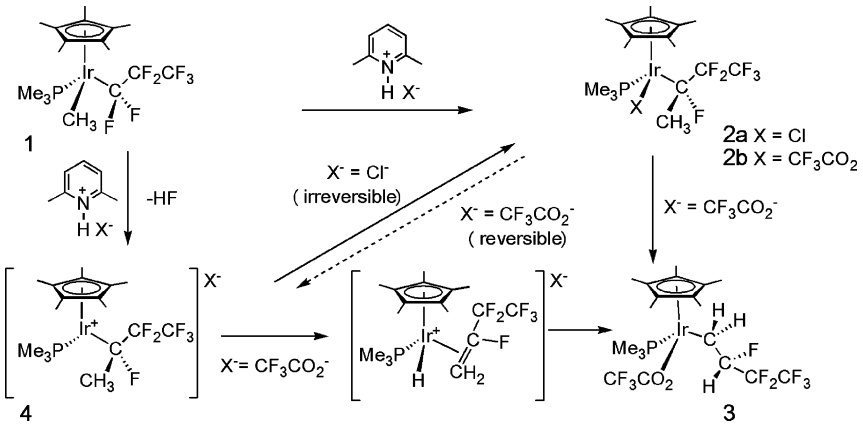

centers bearing fluorine has been of particular interest due to their potential biological applications.[19,30,31] We have sought methodology for the complementary approach, in which C−H and C−C bonds can be generated by substitution at a C−F bond.[32−35] Clearly, the strength of the C−F bond allows synthetic methodology for its production via C−F bond formation chemistry, whether it be via F^- addition to electrophilic carbon or by electrophilic "F^+" addition to nucleophilic carbon centers, to be straightforward, while providing a thermodynamic impediment to the complementary approach involving breaking the C−F bond, which must be compensated for by formation of a strong bond from fluorine to another element.

The question of whether the σ^* orbitals of C−F bonds α to transition metals are capable of acting as π-acceptors, thereby weakening the C−F bond and activating it toward reaction, has long intrigued chemists and is an idea whose appeal has waxed and waned over the years,[36−39] as has its organic equivalent of negative hyperconjugation.[40−43] However, while there are few pieces of evidence for such weakening in spectroscopic or ground state structural studies, it has long been clear that aliphatic C−F bonds are labile toward external Lewis acids when they are α to certain transition metal centers and that C−F bond activation by various exogenous protic acids[44−47] and Lewis acids[48−52] can be achieved quite easily. The recent discovery in our group that the source of the exogenous acid could be heterolytically activated H_2, with resulting hydrogenolysis of α-C−F bonds of fluoroalkyl ligands to liberate environmentally friendly hydrofluorocarbons (HFCs), provided considerable stimulation for more detailed studies of this type of reaction.[32,34]

Even more recently we reported the first apparently diastereoselective α-C−F bond activation, coupled with formation of a C−C bond.[35] Remarkably, instead of undergoing protonation at the metal or at the Ir−CH_3 bond to give methane, the iridium complex **1** reacts with HCl in the form of lutidinium chloride at the α-CF_2 group to give HF in the form of lutidinium fluoride; migration of the methyl group from iridium to the α-carbon generates a new C−C bond and a carbon stereocenter, and subsequent trapping at the metal with the chloride counteranion affords product **2a** (Scheme 1). The diastereoselectivity of this reaction was 100%, and the relative configurations at the α-carbon and at Ir were shown unambiguously to be (R_C,R_{Ir}) or (S_C,S_{Ir}) by X-ray crystallography.[35]

When this reaction was carried out using lutidinium trifluoroacetate, the product was **3**, formed as a 4:1 mixture of diastereomers. Monitoring the reaction by NMR indicated that the initially formed product was indeed **2b**, which then isomerized to **3**. In this case, it was proposed that trifluoroacetate trapped the metal reversibly compared to chloride, allowing eventual β-H elimination from the intermediate cation **4** to occur, with resultant rearrangement as shown in Scheme 1.[35] Clearly the final overall outcome of this reaction, and thus the preservation or destruction of the newly formed carbon stereocenter, depends on the nature of the trapping counteranion. Moreover, even when the migrating group is one incapable of further rearrangement, such as hydride or phenyl, loss of diastereoselectivity in the final product can occur by inversion at iridium if the 16-electron species **4** (or its analogue) has a significant lifetime, by virtue either of slow trapping or of anion dissociation after initial trapping. As a consequence, the clarity of any conclusion whether diastereoselectivity of C−F activation

(26) Togni, A.; Mezzetti, A.; Barthazy, P.; Becker, C.; Devillers, I.; Frantz, R.; Hintermann, L.; Perseghini, M.; Sanna, M. *Chimia* **2001**, *55*, 801−805.
(27) Shibata, N.; Suzuki, E.; Takeuchi, Y. *J. Am. Chem. Soc.* **2000**, *122*, 10728−10729.
(28) Differding, E.; Lang, R. W. *Tetrahedron Lett.* **1988**, *29*, 6087−6090.
(29) Iseki, K. *Tetrahedron* **1998**, *54*, 13887−13914.
(30) Ramachandran, P. V. *ACS Symp. Ser.* **2001**, *746*, 310.
(31) Filler, R. *ACS Symp. Ser.* **2001**, *746*, 1−20.
(32) Hughes, R. P.; Smith, J. M. *J. Am. Chem. Soc.* **1999**, *121*, 6084−6085.
(33) Hughes, R. P.; Lindner, D. C.; Rheingold, A. L.; Liable-Sands, L. M. *J. Am. Chem. Soc.* **1997**, *119*, 11544−11545.
(34) Hughes, R. P.; Willemsen, S.; Williamson, A.; Zhang, D. *Organometallics* **2002**, *21*, 3085−3087.
(35) Hughes, R. P.; Zhang, D.; Zakharov, L. N.; Rheingold, A. L. *Organometallics* **2002**, *21*, 4902−4904.
(36) Graham, W. A. G. *Inorg. Chem.* **1968**, *7*, 315−321.
(37) King, R. B.; Bisnette, M. B. *J. Organomet. Chem.* **1964**, *2*, 15−37.
(38) Cotton, F. A.; McCleverty, J. A. *J. Organomet. Chem.* **1965**, *4*, 490.
(39) Cotton, F. A.; Wing, R. M. *J. Organomet. Chem.* **1967**, *9*, 511−517.
(40) Saunders, W. H. *J. Org. Chem.* **1999**, *64*, 861−865.
(41) Farnham, W. B.; Dixon, D. A.; Calabrese, J. C. *J. Am. Chem. Soc.* **1988**, *110*, 2607−2611.
(42) Dixon, D. A.; Fukunaga, T.; Smart, B. E. *J. Am. Chem. Soc.* **1986**, *108*, 4027−4031.
(43) Dawson, W. H.; Hunter, D. H.; Willis, C. *J. Chem. Soc., Chem. Commun.* **1980**, 874−875.
(44) Appleton, T. G.; Berry, R. D.; Hall, J. R.; Neale, D. W. *J. Organomet. Chem.* **1989**, *364*, 249−273.
(45) Clark, G. R.; Hoskins, S. V.; Roper, W. R. *J. Organomet. Chem.* **1982**, *234*, C9−C12.
(46) Burrell, A. K.; Clark, G. R.; Rickard, C. E. F.; Roper, W. R. *J. Organomet. Chem.* **1994**, *482*, 261−269.
(47) Michelin, R. A.; Ros, R.; Guadalupi, G.; Bombieri, G.; Benetollo, F.; Chapuis, G. *Inorg. Chem.* **1989**, *28*, 840−846.
(48) Koola, J. D.; Roddick, D. M. *Organometallics* **1991**, *10*, 591−597.
(49) Crespi, A. M.; Shriver, D. F. *Organometallics* **1985**, *4*, 1830−1835.
(50) Richmond, T. G.; Crespi, A. M.; Shriver, D. F. *Organometallics* **1984**, *3*, 314−319.
(51) Richmond, T. G.; Shriver, D. F. *Organometallics* **1984**, *3*, 305−314.
(52) Reger, D. L.; Dukes, M. D. *J. Organomet. Chem.* **1978**, *153*, 67−72.

Scheme 2

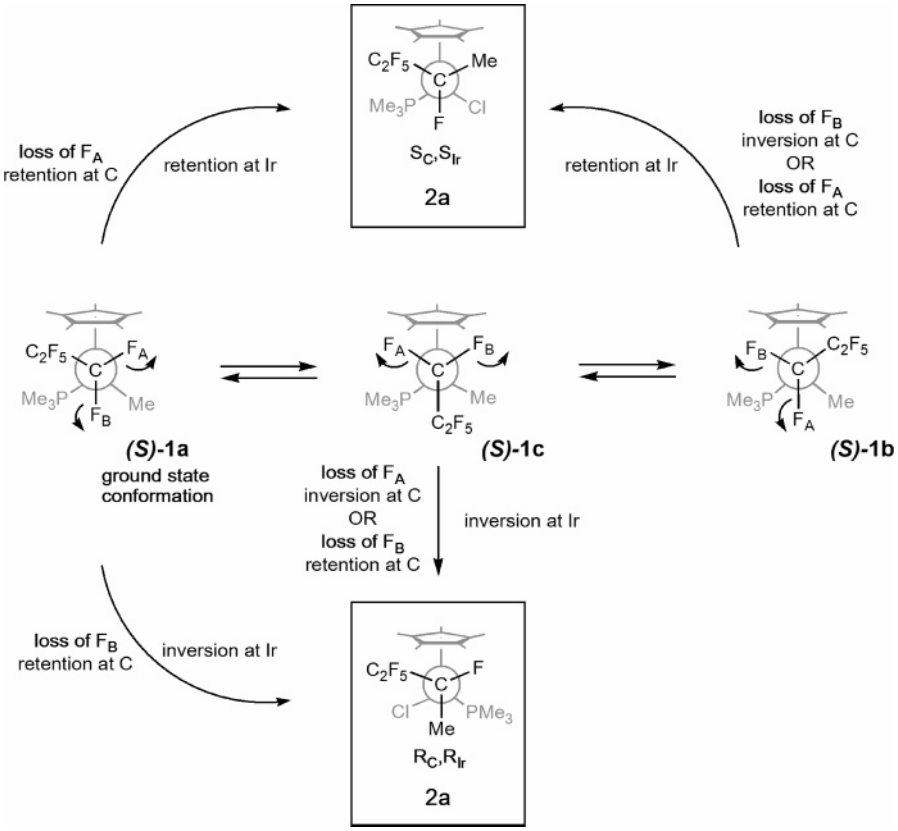

at carbon is itself 100% in all cases can be muddied by subsequent inversion or ligand rearrangement chemistry involving the metal center.

As mentioned, the relative configurations of the Ir and C stereocenters of **2a** have been firmly established as (R_C,R_{Ir}) or (S_C,S_{Ir}) by X-ray crystallography.[35] Unhappily, this relative stereochemistry in the product can be afforded via six stereochemically distinct pathways for the sequence of C−F bond activation and C−C bond formation, followed by counterion trapping with either retention or inversion at the iridium stereocenter. These are shown in Scheme 2 as evolving from the three staggered conformations of the *S*-enantiomer of **1**, each of which is viewed as a Newman projection down the C−Ir bond. The observed ground state conformation of **1**, in the solid state and in solution, is that shown as **1a** in Scheme 2. For example, completely diastereoselective protonation of F_A from conformation **(*S*)-1a**, followed by (or concomitant with) migration of the methyl with retention at carbon, followed in turn by trapping by chloride with retention at iridium, affords the correct (S_C,S_{Ir}) configuration. Likewise, completely diastereoselective protonation of F_B from conformation **(*S*)-1a**, methyl migration with retention at carbon, and chloride trapping with inversion at iridium affords the indistinguishable (R_C,R_{Ir}) enantiomer. Two analogous pathways from conformer **(*S*)-1b**, both of which generate the observed relative (S_C,S_{Ir}) stereochemistry, are shown in Scheme 2. An additional pathway is also available from conformation **(*S*)-1c**, but this must lead to the (R_C,R_{Ir}) enantiomer of the product, as shown in Scheme 2. Unfortunately, therefore, the information available regarding the relative stereochemistries at C and Ir cannot address the question of individual diastereoselectivities at either atom, as the observed relative stereochemistry in the product can be obtained via six indistinguishable pathways, three of which must proceed with net inversion at iridium.

To eliminate those pathways involving inversion at iridium, it was decided to design a reaction in which the migrating group could act as an intramolecular trap at the metal immediately after formation of the new C−C bond and new carbon stereocenter, thereby effectively guaranteeing that it would trap at the metal from the same side as it attacked the α-carbon; that is, the reaction would have to proceed with retention at the metal. The vinyl derivative **5** was deemed a likely prospect, and to this end its synthesis and chemistry were examined and are described herein.

Results and Discussion

The desired vinyl complex **5** was prepared by addition of an

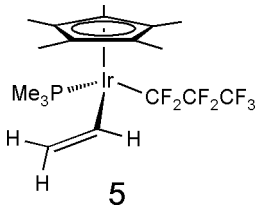

5

ethereal solution of vinyllithium[53] to a suspension of Cp*Ir(PMe$_3$)($CF_2CF_2CF_3$)OTf[35] in ether at −78 °C. Crystals of **5** suitable for X-ray diffraction were obtained by slow evaporation of a hexane solution in the absence of air. Details of this crystallographic determination, and of others described later in this paper, are given in Table 1. An ORTEP diagram of **5** is shown in Figure 1. In the solid state, the vinyl group is positioned

(53) Seyferth, D.; Weiner, M. A. *J. Am. Chem. Soc.* **1961**, *83*, 3583−3586.

Table 1. Crystal, Data Collection, and Refinement Parameters for Compounds **5**, **6**, and **8**

	5	**6**	**8**
formula	$C_{18}H_{27}F_7IrP$	$C_{18}H_{27}F_6IIrP$	$C_{50}H_{38}BF_{30}IrP$
fw	599.57	707.47	1442.78
space group	*P*2(1)/*n*	*P*2(1)/*c*	$P\bar{1}$
a, Å	8.7408(5)	14.8066(11)	12.1256(9)
b, Å	25.7847(14)	9.0186(7)	12.5665(9)
c, Å	9.2802(5)	16.9374(12)	18.2649(13)
α, deg	90	90	84.3880(10)
β, deg	103.9830(10)	103.5590(10)	73.3670(10)
γ, deg	90	90	84.6180(10)
V, Å^3	2029.58(19)	2198.7(3)	2647.6(3)
Z	4	4	2
cryst color, habit	yellow, plate	orange, block	colorless, block
D(calcd), g/cm^3	1.962	2.137	1.810
μ(Mo Kα), mm^{-1}	6.719	7.600	2.694
temp, K		100(2)	
diffractometer		Bruker Smart Apex CCD	
radiation		Mo Kα ($\lambda = 0.71073$ Å)	
measd reflns	12526	13214	22728
indep reflns	4612 [$R_{int} = 0.0227$]	4950 [$R_{int} = 0.0331$]	11 762 [$R_{int} = 0.0215$]
$R(F)$ [$I > 2\sigma(I)$], %[a]	2.25	2.59	5.27
$R(wF^2)$ [$I > 2\sigma(I)$], %[a]	5.34	5.64	11.83

[a] $R = \sum||F_o| - |F_c||/\sum|F_o|$; $R(wF^2) = \{\sum[w(F_o^2 - F_c^2)^2]/\sum[w(F_o^2)^2]\}^{1/2}$; $w = 1/[\sigma^2(F_o^2) + (aP)^2 + bP]$, $P = [2F_c^2 + \max(F_o,0)]/3$.

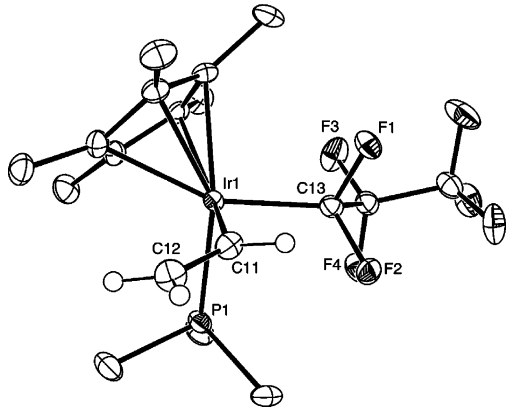

Figure 1. ORTEP diagram for **5** with ellipsoids drawn at the 30% probability level. Hydrogen atoms are excluded, with the exception of those on the vinyl ligand. Selected bond lengths (Å) and angles (deg): Ir(1)−C(11), 2.067(3); Ir(1)−C(13), 2.062(3); Ir(1)−P(1), 2.2627(9); Ir(1)−Cp(cent), 1.920(5); C(11)−C(12), 1.322(5); C(13)−F(1), 1.406(4); C(13)−F(2), 1.398(4); C(13)−Ir(1)−C(11), 83.59(13); C(13)−Ir(1)−P(1), 93.06(10); C(11)−Ir(1)−P(1), 86.51(10); C(12)−C(11)−Ir(1), 127.9(3); F(2)−C(13)−F(1), 101.6(2); F(3)−C(14)−F(4), 107.0(3).

conveniently for migration as the vinylic CH_2 terminus is oriented away from the perfluoropropyl group. To examine the preferred conformation of **5** in solution, $^{19}F\{^1H\}$ HOESY (heteronuclear Overhauser effect spectroscopy) techniques were employed.[54] For molecules containing ^1H and ^{19}F nuclei this methodology can provide information about the relative spatial orientation of groups containing these nuclei in solution, with a cross-peak observed if two nuclei are close in space (≤5 Å).[55] It has been extensively used in studying transition metal ion-pair interactions in solution,[56−64] and we have recently reported its use in organometallic analogues of **2** and **5**, in which the solution state conformations can be deduced from the NOE interactions between fluorine atoms of the perfluoroalkyl ligand and the protons of Cp*, PMe_3, and other ligands.[54] The $^{19}F\{^1H\}$ HOESY spectrum of **5** is shown in Figure 2; the only solution conformation consistent with the observed cross-peaks is illustrated in the same figure as a Newman projection viewed along the CF_2−Ir bond. The preferred solution conformation is clearly the same as that found in the solid state (vide supra).

It was initially anticipated that reaction of compound **5** with HI in the form of 2,6-lutidinium iodide would result in α-C−F bond activation followed by vinyl group migration to give an η^1-allyl intermediate, followed by rapid intramolecular closure to give an η^3-allylic ligand, thereby freezing the stereochemistry at the fluorinated carbon. Instead, the reaction afforded the rearranged η^1-allyl complex **6** (Scheme 3), which was isolated and fully characterized by X-ray crystallography and spectroscopy. An ORTEP representation of the structure is shown in Figure 3. In addition to characteristic Cp* and PMe_3 peaks, the ^1H NMR spectrum of **6** shows the two diastereotopic α-hydrogens as multiplets at 2.36 and 3.11 ppm, with the *β*-hydrogen appearing at 5.76 ppm as a doublet of doublets of doublets from coupling to two hydrogens and the *trans*-fluorine atom. The ^{19}F NMR spectrum shows the CF_3 as a doublet of triplets, an AB quartet due to the diastereotopic fluorine atoms of the CF_2 group, and a broad multiplet due to the single vinylic fluorine.

When the reaction was monitored by ^1H NMR spectroscopy, a complex mixture of intermediates was observed, which evolved over a period of several hours at room temperature to give clean signals for the final product **6**. Unfortunately the spectra of these intermediate species have proven difficult to decipher, and all the desired information about diastereoselec-

(54) Hughes, R. P.; Zhang, D.; Ward, A. J.; Zakharov, L. N.; Rheingold, A. L. *J. Am. Chem. Soc.* **2004**, *126*, 6169−6178.
(55) Neuhaus, D.; Williamson, M. P. *The Nuclear Overhauser Effect in Structural and Conformational Analysis*; Wiley-VCH: New York, 2000.
(56) Macchioni, A.; Romani, A.; Zuccaccia, C. *Organometallics* **2003**, *22*, 1526−1533.
(57) Macchioni, A. *Eur. J. Inorg. Chem.* **2003**, 195−205.
(58) Kumar, P. G. A.; Pregosin, P. S.; Goicoechea, J. M.; Whittlesey, M. K. *Organometallics* **2003**, *22*, 2956−2960.
(59) Burini, A.; Fackler, J. P.; Galassi, R.; Macchioni, A.; Omary, M. A.; Rawashdeh-Omary, M. A.; Pietroni, B. R.; Sabatini, S.; Zuccaccia, C. *J. Am. Chem. Soc.* **2002**, *124*, 4570−4571.
(60) Zuccaccia, C.; Bellachioma, G.; Cardaci, G.; Macchioni, A. *J. Am. Chem. Soc.* **2001**, *123*, 11020−11028.
(61) Macchioni, A.; Zuccaccia, C.; Clot, E.; Gruet, K.; Crabtree, R. H. *Organometallics* **2001**, *20*, 2367−2373.
(62) Bellachioma, G.; Cardaci, G.; Macchioni, A.; Valentini, F.; Zuccaccia, C.; Foresti, E.; Sabatino, P. *Organometallics* **2000**, *19*, 4320−4326.
(63) Zuccaccia, C.; Macchioni, A.; Orabona, I.; Ruffo, F. *Organometallics* **1999**, *18*, 4367−4372.
(64) Macchioni, A.; Bellachioma, G.; Cardaci, G.; Gramlich, V.; Rueegger, H.; Terenzi, S.; Venanzi, L. M. *Organometallics* **1997**, *16*, 2139−2145.

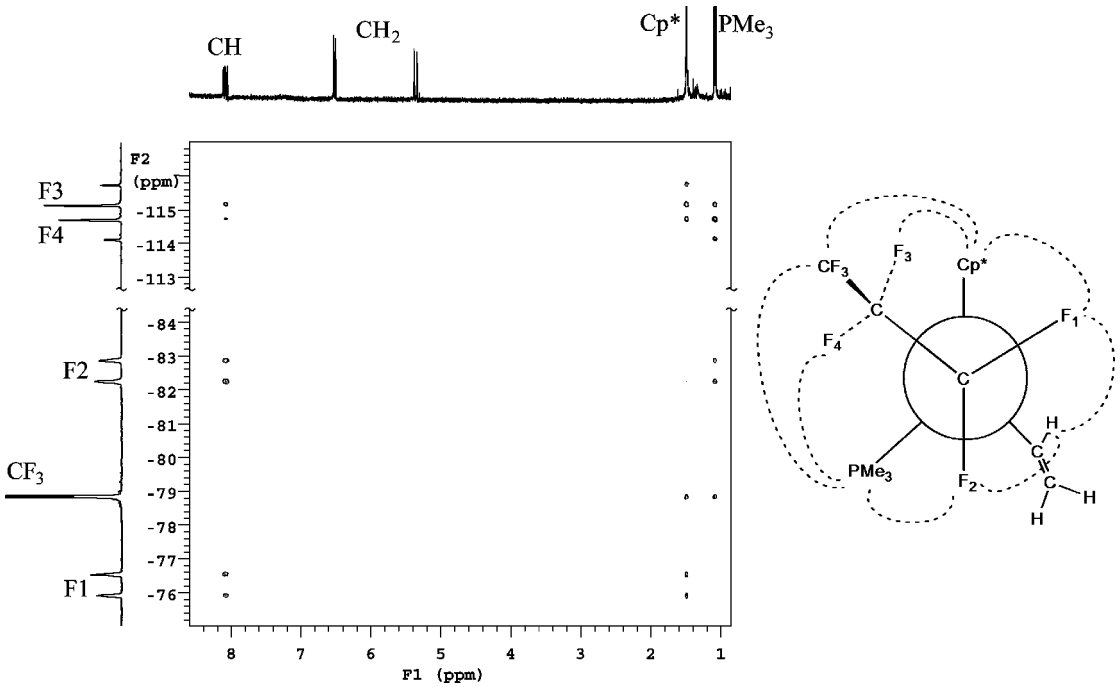

Figure 2. $^{19}F\{^1H\}$ HOESY spectrum for **5** in C_6D_6 (mixing time 3.0 s) and the solution conformation of **5** deduced from this spectrum. (The curved lines show the observed NOE interactions.)

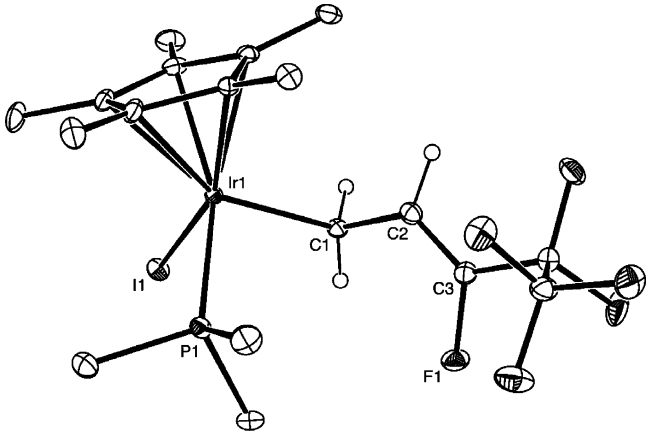

Figure 3. ORTEP diagram for **6** with ellipsoids drawn at the 30% probability level. Selected hydrogen atoms are excluded. Selected bond lengths (Å): Ir(1)−C(1), 2.147(4); Ir(1)−P(1), 2.2591(11); Ir(1)−I(1), 2.7112(3); Ir(1)−Cp(cent), 1.861(5); C(1)−C(2), 1.485(6); C(2)−C(3), 1.319(6); C(3)−F(1), 1.368(5). C(1)−Ir(1)−P(1), 90.97(12); C(1)−Ir(1)−I(1), 86.05(11); P(1)−Ir(1)−I(1), 87.52(3).

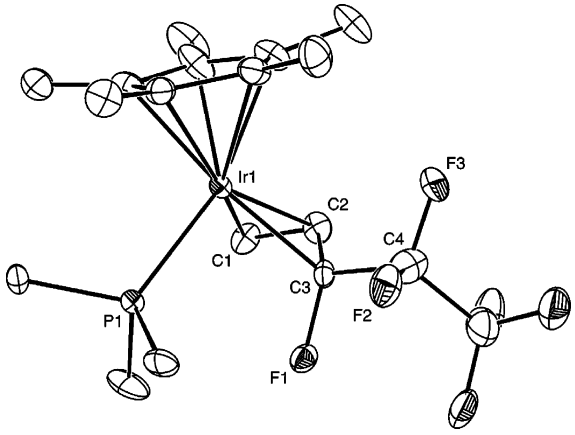

Figure 4. ORTEP diagram for cation of **8** with ellipsoids drawn at the 30% probability level. All hydrogen atoms are excluded. Selected bond lengths (Å) and angles (deg): Ir(1)−P(1), 2.3180(16); Ir(1)−C(1), 2.191-(7); Ir(1)−C(2), 2.106(7); Ir(1)−C(3), 2.144(7); Ir(1)−Cp(cent), 1.854(5); C(1)−C(2), 1.415(11); C(2)−C(3), 1.436(10); C(3)−F(1), 1.378(11); C(1)−C(2)−C(3), 115.5(7); C(2)−C(3)−C(4), 119.6(6); C(2)−C(3)−F(1), 116.6-(6).

tivity of the vinyl migration is lost via allylic rearrangement and coordination of iodide. In an attempt to circumvent these problems, the reaction was repeated using lutidinium tetrakis-[3,5-bis(trifluoromethyl)phenyl]borate $[LutH^+B(ArF)_4^-]$[65] containing a weakly coordinating counteranion.

Reaction of **5** with $[LutH^+B(ArF)_4^-]$ in CD_2Cl_2 at room temperature was complete within seconds to give a mixture of η^3-allylic complexes, shown to be the *exo-anti* isomer **7** and *exo-syn*-isomer **8** in a ratio of 5.7:1 (Scheme 4). On standing in solution at room temperature for several hours *exo-anti*-**7** completely rearranged into *exo-syn*-**8**, which is clearly and unambiguously the thermodynamically preferred η^3-allylic isomer. We note that the preferred *exo*-orientation of this η^3-allylic ligand is quite unusual; in similar rhodium[66] and iridium[67] systems containing the parent η^3-allyl ligand, the *endo*-orientation is thermodynamically preferred. As expected, reaction of compound **8** with iodide affords the previously characterized compound **6**.

The thermodynamic isomer **8** was isolated as pale yellow crystals and was completely characterized by ^1H, ^{19}F, and ^{31}P NMR spectroscopy, microanalysis, and X-ray crystallography. The crystal structure of the cationic portion of **8**, along with selected bond lengths and angles, is shown in Figure 4. The

(65) Yandulov, D. V.; Schrock, R. R. *J. Am. Chem. Soc.* **2002**, *124*, 6252−6253.

(66) Periana, R. A.; Bergman, R. G. *J. Am. Chem. Soc.* **1986**, *108*, 7346−7355.
(67) McGhee, W. D.; Bergman, R. G. *J. Am. Chem. Soc.* **1988**, *110*, 4246−4262.

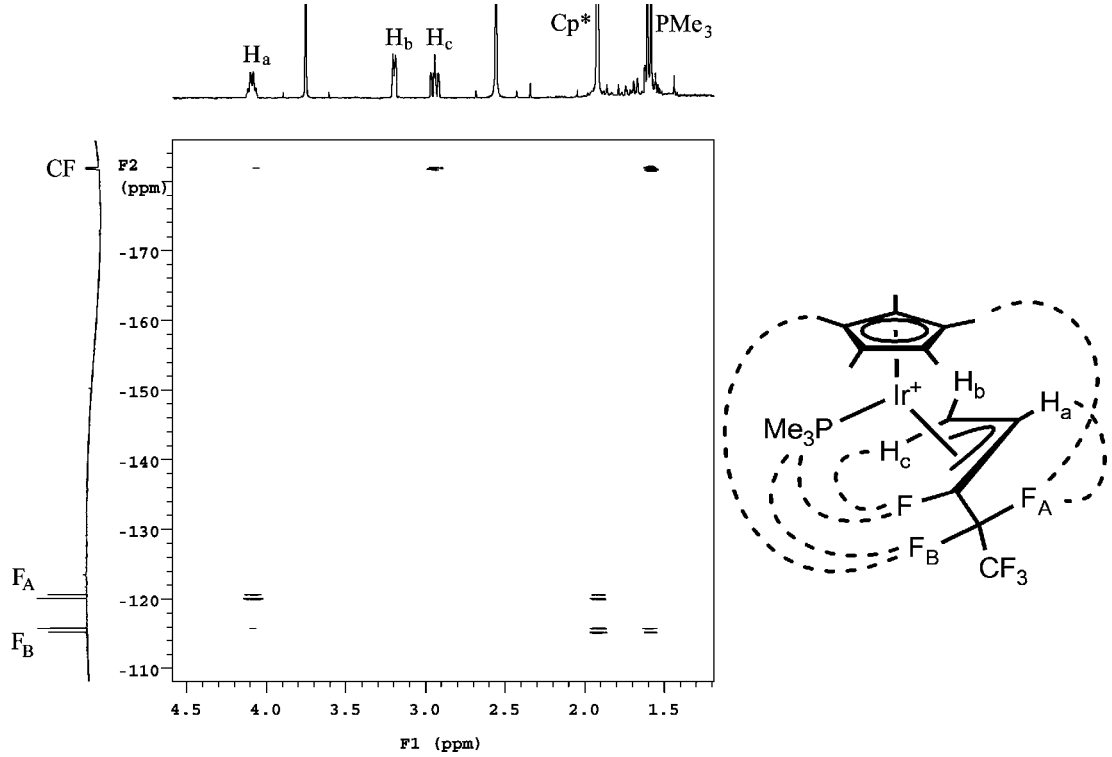

Figure 5. $^{19}F\{^1H\}$ HOESY spectrum for **8** in CD_2Cl_2 (mixing time 3.0 s) and the solution conformation of **8** deduced from the spectrum. (The curved lines show the observed NOE interactions; additional $^1H/^1H$ NOE interactions are described in the text.)

Scheme 3

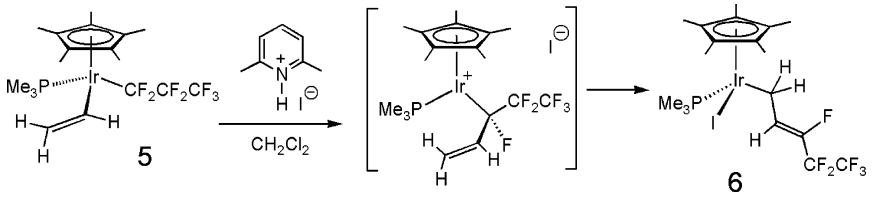

Scheme 4

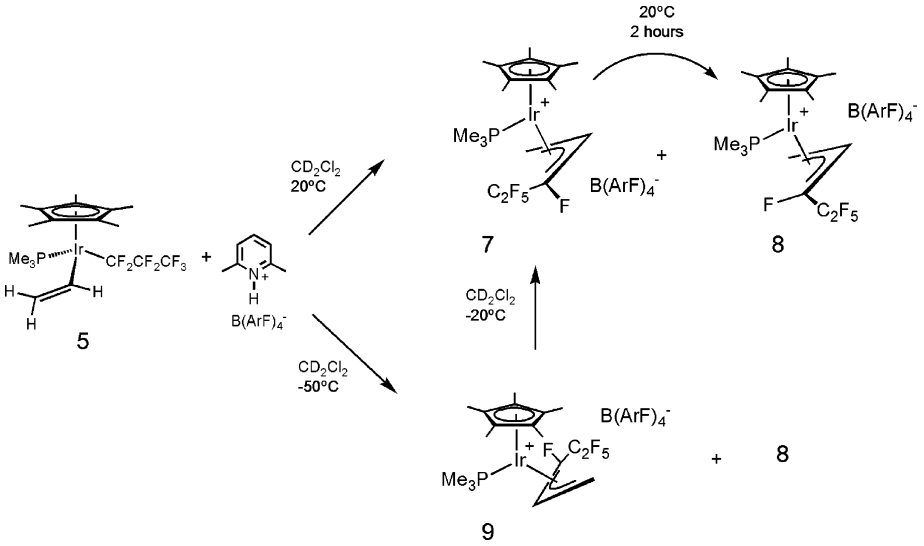

solution structure of **8** was shown to be *exo-syn*, consistent with that in the solid state, using $^{19}F\{^1H\}$ HOESY (Figure 5) and 1D $^1H,^1H$ NOESY experiments. The latter experiment showed that the H_a proton has an NOE interaction with Cp* but not with PMe_3. No attempts were made to use this technique to measure specific distances as others have done.[57,60] Here we are concerned only with determining relative proximities to afford a rapid, yet unambiguous, determination of solution conformation and configuration. The structure of **7** was likewise unequivocally established by the results of $^{19}F\{^1H\}$ HOESY

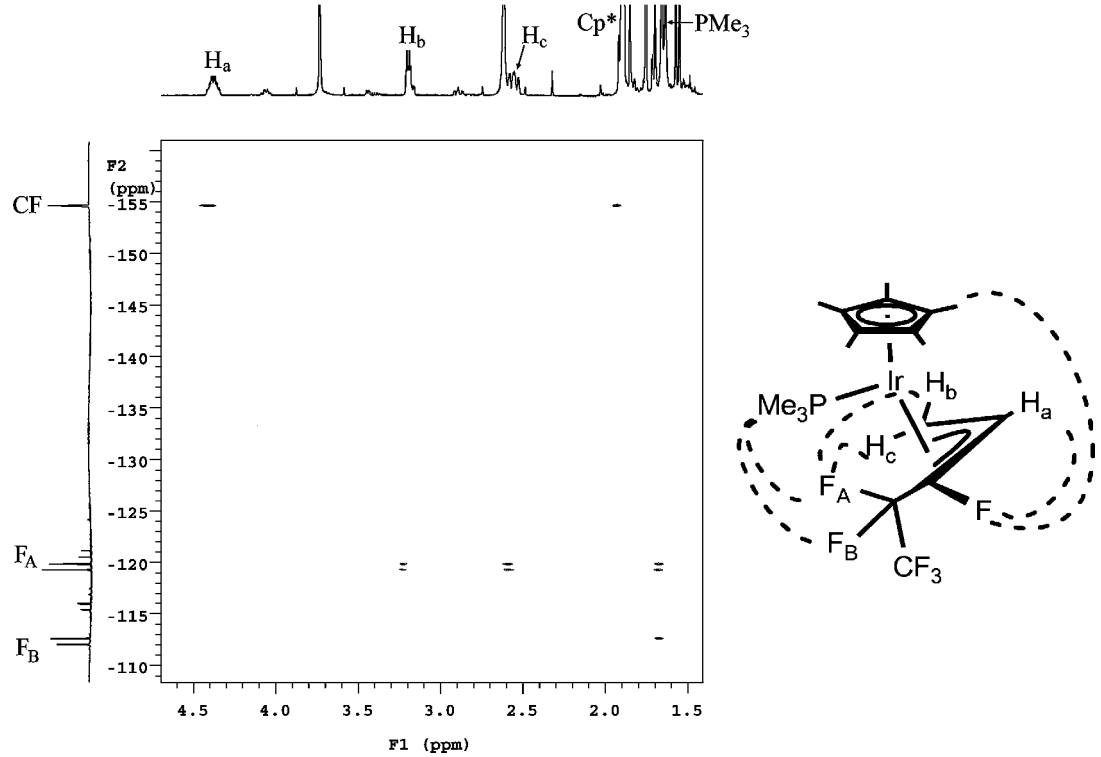

Figure 6. $^{19}F\{^1H\}$ HOESY spectrum for **7** in CD_2Cl_2 (mixing time 3.0 s) and the solution conformation of **7** deduced from the spectrum. (The curved lines show the observed NOE interactions; additional $^1H/^1H$ NOE interactions are described in the text.)

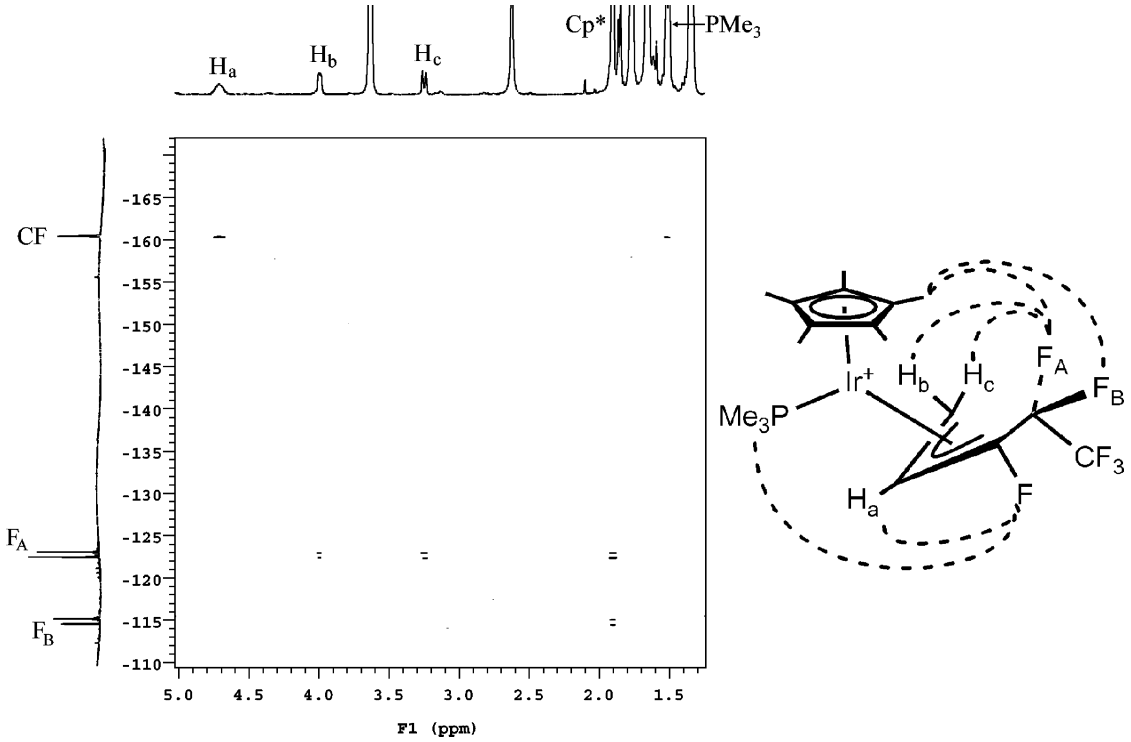

Figure 7. $^{19}F\{^1H\}$ HOESY spectrum for **9** in CD_2Cl_2 (mixing time 3.0 s) and the solution conformation of **9** deduced from the spectrum. (The curved lines show the observed NOE interactions; additional $^1H/^1H$ NOE interactions are described in the text.)

(Figure 6) and 1D $^1H,^1H$ NOESY experiments. Once again the latter experiment showed that the H_a proton has an NOE interaction with Cp* but not with PMe_3.

However, compounds **7** and **8** observed and isolated at room temperature are not the true kinetic products of the C−F activation/vinyl migration reaction, which are revealed by the reaction of **5** with $[LutH^+B(ArF)_4^-]$ at −50 °C. At this temperature the only two products observed by ^1H and ^{19}F NMR spectroscopy are **8** and the previously unobserved *endo-anti*-isomer **9**, in a ratio of 1:8 (Scheme 4). As with its previously described isomers, structural characterization of **9** was firmly established by $^{19}F\{^1H\}$ HOESY (Figure 7) and 1D $^1H,^1H$

Scheme 5

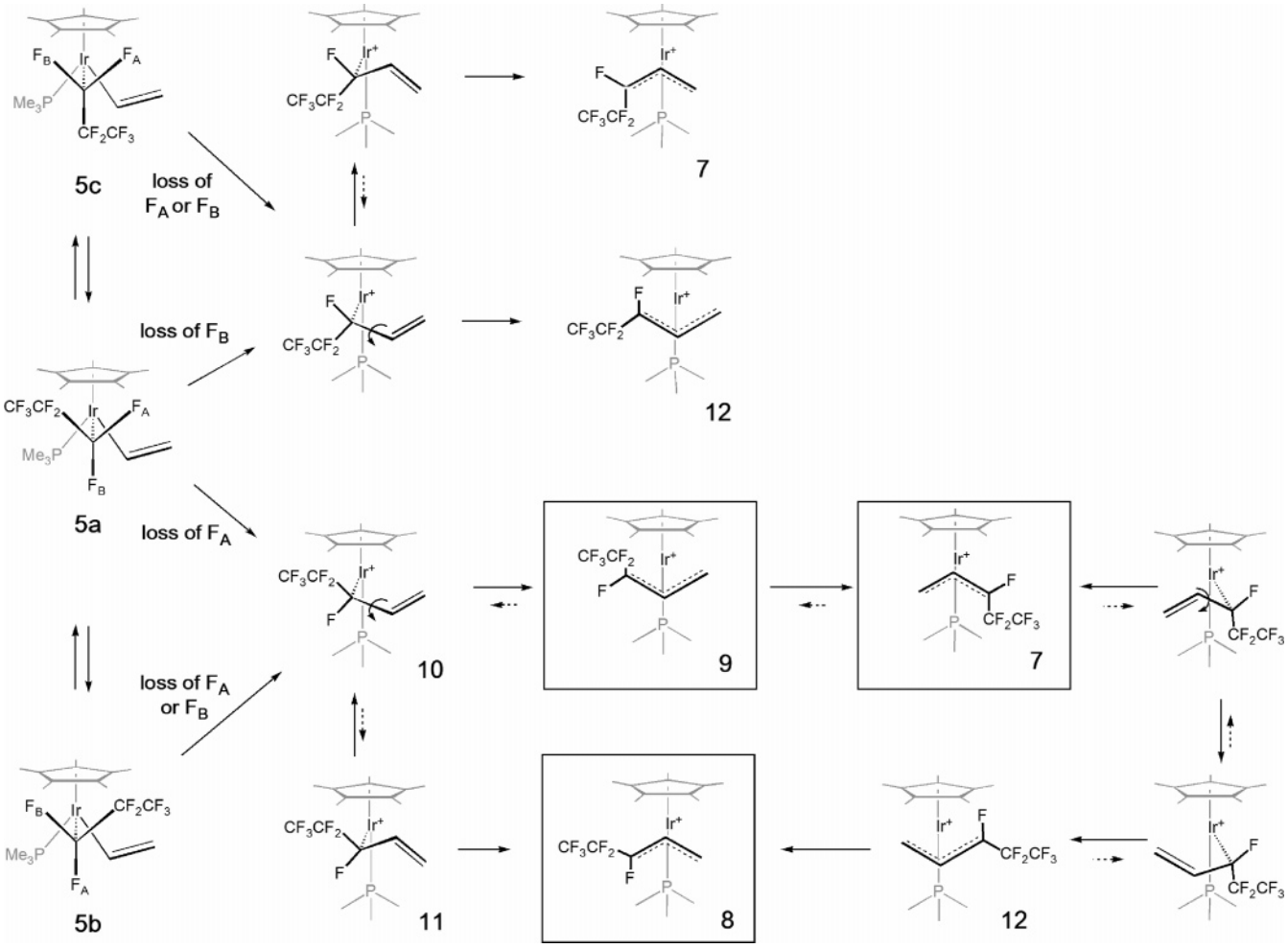

NOESY experiments at low temperature. The *anti* arrangement of the C_2F_5 substituent on the allyl ligand is evident from the observed HOESY cross-peaks between F_A of the CF_2 unit and both terminal hydrogens of the allyl ligand and a strong interaction between the allylic C−F fluorine and H_a. The *endo* orientation of the allyl ligand is suggested by the observed HOESY interactions of both CF_2 fluorines with Cp* hydrogens and the allylic C−F fluorine with the PMe_3 hydrogens and confirmed by a 1D $^1H,^1H$ NOESY experiment, which showed an interaction of H_a with the PMe_3 but not with Cp*.

On warming the solution to −20 °C, the resonances of **9** rapidly evolve into those of **7** and, on warming to 20 °C, eventually into those of the thermodynamic isomer **8**. Thus, compound **7** does not arise directly from migration of the vinyl group in compound **5**, but is formed by rearrangement of *endo-anti*-isomer **9** presumably by rotation around the Ir−allyl bond or an $\eta^3 \rightarrow \eta^1 \rightarrow \eta^3$ rearrangement of the allylic ligand.[68−71] This transformation is sufficiently rapid so that **9** is not observed at −20 °C or above.

As a result, the products that truly reveal the stereochemistry of the C−F-activation/vinyl-migration reaction, and whose structures must be accommodated by the mechanism, are *exo-syn*-**8** and *endo-anti*-**9**, with the latter being by far the dominant product. The small amount of **8** formed kinetically at −50 °C cannot arise via intermediate **7**, which is stable to isomerization at this temperature. Consequently the kinetic reaction pathway must be one that generates **9** as the principal kinetic product, but also accounts for the formation of small amounts of **8** without the intermediacy of **7**.

Scheme 5 illustrates two pathways emanating from the ground state conformation of **5**, shown as **5a**. Diastereoselective loss of F_A and vinyl migration affords η^1-allylic intermediate **10**, rapid closure of which affords the observed major diastereomer **9**. Rotation within the η^1-allyl bond in **10** before closure can afford **11**, which in turn generates the observed small amount of diastereomer **8**. We cannot discount that **10** and **11** are formed directly by competitive migration from two different conformations of the vinyl ligand itself, with concerted formation of the η^3-allyl species, and indeed there is some support for avoidance of coordinatively unsaturated intermediates when a concerted reaction is possible.[72] However, this does not affect any arguments concerning the stereochemistry of C−F bond activation. At higher temperatures **9** evolves to **7** and eventually to **8** as shown in Scheme 5. Notably diastereomer **12** is the only η^3-allyl isomer not observed spectroscopically. Formation of **8**

(68) Faller, J. W.; Incorvia, M. J. *J. Organomet. Chem.* **1969**, *19*, P13−P16.
(69) Blom, R.; Swang, O. *Eur. J. Inorg. Chem.* **2002**, 411−415.
(70) Guerrero, A.; Jalon, F. A.; Manzano, B. R.; Rodriguez, A.; Claramunt, R. M.; Cornago, P.; Milata, V.; Elguero, J. *Eur. J. Inorg. Chem.* **2004**, 549−556.
(71) Xue, P.; Bi, S.; Sung, H. H. Y.; Williams, I. D.; Lin, Z.; Jia, G. *Organometallics* **2004**, *23*, 4735−4743.
(72) Casey, C. P.; Vosejpka, P. C.; Underiner, T. L.; Slough, G. A.; Gavney, J. A., Jr. *J. Am. Chem. Soc.* **1993**, *115*, 6680−6688.

Scheme 6

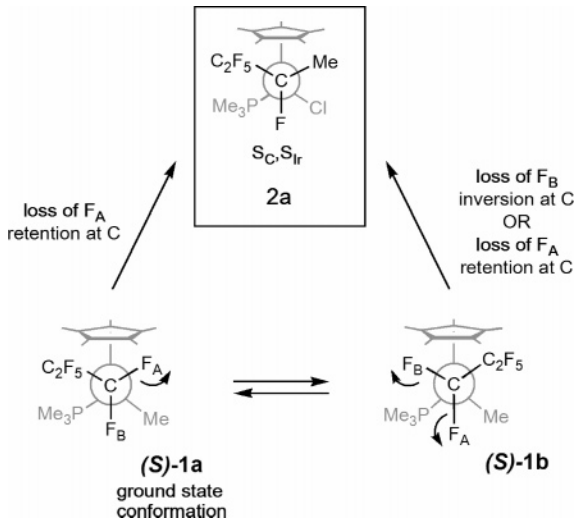

from **7** either requires **7** to revert to **9** before conversion to **8**, or it must pass through **12** en route to **8**. If the latter pathway pertains, since conversion of **9** → **7** is fast at −20 °C, and since **7** converts to **8** only slowly at room temperature, it seems consistent that the allylic rotation or $\eta^3 \rightarrow \eta^1 \rightarrow \eta^3$ rearrangement that converts **12** → **8** is considerably faster than formation of **12** from **7**, so that no significant observable concentration of **12** is formed above −20 °C. Notably, while loss of F_A from **5a** affords the observed kinetic diastereomers, diastereoselective activation of F_B from this conformation must lead to formation of **12** and **7**, neither of which is observed as a kinetic product at −50 °C. Similarly, activation of either F_A or F_B from conformation **5c** cannot afford the observed kinetic products. In contrast, activation of either F_A or F_B from conformation **5b** can afford the observed kinetic products.

Given that this reaction precludes formation of products arising from inversion at iridium, at least under conditions of true kinetic control, the options for the selectivity of C−F bond activation are narrowed to those three pathways shown in Scheme 5 that afford **9** and **8**. Provided that these conclusions pertain to other analogous migrating groups such methyl, and thus excluding all pathways leading to the observed diastereomers that require inversion at iridium, the six pathways shown in Scheme 2 are reduced to the three illustrated in Scheme 6, which originate from only two possible conformations of the fluoroalkyl ligand. It would be a remarkable coincidence if more than one of these three pathways is operative, since each appears to have quite different steric requirements for approach of the acid to the α-fluorine and for methyl migration. We conclude, therefore, that C−F activation by exogenous acid and formation of the new carbon stereocenter in these systems involve a completely diastereoselective pathway, a conclusion also required by application of Occam's razor.

Further studies are underway with a view to establishing enantioselective transformations based on this chemistry and to better understanding of the mechanistic details of this unusual reaction type.

Experimental Section

General Considerations. Air-sensitive reactions were performed in oven-dried glassware, using standard Schlenk techniques, under an atmosphere of nitrogen, which was deoxygenated over BASF catalyst and dried over Aquasorb, or in an MBraun drybox. Methylene chloride, hexanes, diethyl ether, tetrahydrofuran, and toluene were dried over an alumina column under nitrogen.[73] NMR spectra were recorded on a Varian Unity Plus 300 or 500 FT spectrometer. ^{1}H NMR spectra were referenced to the protio impurity in the solvent: C_6D_6 (7.15 ppm), CD_2Cl_2 (5.32 ppm). ^{19}F NMR spectra were referenced to external $CFCl_3$ (0.00 ppm). ^{31}P{^{1}H} NMR spectra were referenced to 85% H_3PO_4 (0.00 ppm). Coupling constants are reported in units of hertz. Elemental analyses were performed by Schwartzkopf (Woodside, NY). Cp*Ir(PMe$_3$)($CF_2CF_2CF_3$)OTf[35] and LiCH=CH_2[53] were prepared according to literature procedures.

Monitoring by ^{1}H NMR Spectroscopy. The migration reactions were monitored in the probe of a Varian Unity Plus 500 spectrometer at temperatures in the range −60 to 35 °C. Each starting compound was dissolved to 0.65−0.75 mL of solution, and a sample was transferred to a J. Young's NMR tube and placed in the NMR probe. For reactions carried out at low temperature, the reaction mixture was prepared in an NMR tube on a Schlenk line in a −78 °C cold bath and then placed in the NMR probe at the appropriate temperature. 1,3,5-Trimethoxybenzene was used as an internal integration standard.

Cp*Ir(PMe$_3$)(*n*-C_3F_7)(CH=CH_2) (5). To a suspension of Cp*Ir(PMe$_3$)(*n*-C_3F_7)OTf (100 mg, 0.138 mmol) in dry ether (∼10 mL) was added a 0.1 M solution of CH_2=CHLi in ether (2 mL, 0.2 mmol) all at once at −78 °C. The resultant yellow solution was stirred for 20 min at −78 °C and warmed to room temperature. The solvent was removed in vacuo, the product extracted with hexanes at room temperature, and the hexanes solution filtered through Celite under an atmosphere of nitrogen. Removal of the hexanes afforded a colorless oil, which crystallized within an hour to give pure product (60 mg, 72%).

Anal. Calcd for $C_{18}H_{27}F_7IrP$: C, 36.06; H, 4.54. Found: C, 35.95; H, 4.91. ^{1}H NMR (C_6D_6 300 MHz, 22 °C): δ 1.09 (d, $^2J_{HP}$ = 10.2 Hz, 9H, PMe$_3$), 1.50 (d, $^4J_{HP}$ = 1.8 Hz, 15H, Cp*), 5.37 (ddd, $^4J_{HP}$ = 2.1 Hz, $^2J_{gem-HH}$= 2.1 Hz, $^3J_{trans-HH}$ = 18.0 Hz, 1H, CH_2, cis to Ir−C), 6.53 (ddd, $^4J_{HP}$ = 2.1 Hz, $^2J_{gem-HH}$ = 2.1 Hz, $^3J_{cis-HH}$ = 10.2 Hz, 1H, CH_2, trans to Ir−C), 8.09 (ddd, $^3J_{HP}$ = 2.1 Hz, $^3J_{cis-HH}$ = 10.2 Hz, $^3J_{trans-HH}$ = 18.0 Hz, 1H, CH). ^{19}F NMR (C_6D_6 282 MHz, 22 °C): δ −76.16 (br d, $^2J_{FF}$ = 292 Hz, 1F, α-CF_2), −78.85 (t, $^3J_{FF}$ = 12.4 Hz, 3F, CF_3) −82.50 (br d, $^2J_{FF}$ = 292 Hz, 1F, α-CF_2), −114.25 (d, $^2J_{FF}$ = 273 Hz, 1F, β-CF_2), −115.55 (d, $^2J_{FF}$ = 273 Hz, 1F, β-CF_2). ^{31}P{^{1}H} NMR (C_6D_6, 121.4 MHz, 22 °C): δ −36.75 (t, $^3J_{PF}$ = 8.4 Hz, 1P, PMe$_3$).

Cp*Ir(PMe$_3$)((*Z*)-CH_2CH=CFC_2F_5)I (6). Cp*Ir(PMe$_3$)(*n*-C_3F_7)(CH=CH_2) (**5**) (50 mg, 0.083 mmol) and lutidinium iodide (19.6 mg, 0.083 mmol) were dissolved in CH_2Cl_2 (∼5 mL) in a Schlenk flask. After 10 h of stirring at room temperature the solution became yellow. The solvent was removed in vacuo, and the product extracted with hexanes. The solution was filtered, and upon slow removal of hexanes by static evaporation orange crystals suitable for X-ray analysis were obtained, (55.7 mg, 95%).

Anal. Calcd for $C_{18}H_{27}F_6IIrP$: C, 30.56; H, 3.85. Found: C, 30.86; H, 3.91. ^{1}H NMR (CD_2Cl_2 500 MHz, 21 °C): δ 1.635 (d, $^2J_{PH}$ = 10.0 Hz, 9H, PMe$_3$), 1.80 (d, $^2J_{PH}$ = 2.0 Hz, 15H, Cp*), 2.36 (dddqd, $^3J_{HH}$ = 7.5 Hz, $^3J_{PH}$ = 7.3 Hz, $^2J_{HH}$ = 7.0 Hz, $^6J_{FH}$ = 3.3 Hz, $^4J_{FH}$ = 2.7 Hz, 1H, CH_2), 3.11 (dddm, $^3J_{HH}$= 10.5 Hz, $^2J_{HH}$ = 7.0 Hz, $^3J_{PH}$ = 4.1 Hz, 1H, CH_2), 5.76 (ddd, $^3J_{FH}$ = 36.5 Hz, $^3J_{HH}$ = 10.5 Hz, $^3J_{HH}$ = 7.5 Hz, 1H, CH). ^{19}F NMR (CD_2Cl_2, 470.3 MHz, 21 °C): δ −84.23 (dt, $^4J_{FF}$ = 7.4 Hz, $^3J_{FF}$ = 3.3 Hz, 3F, CF_3), −119.26 (dm, $^2J_{F(AB)}$ = 278 Hz, 1F, CF_2), −119.40 (dm, $^2J_{F(AB)}$ = 278 Hz, 1F, CF_2), −144.78 (dddqdd, $^3J_{HF}$ = 36.5 Hz, $^3J_{FF}$ = 17.6 Hz, $^3J_{FF}$ = 17.6 Hz, $^4J_{FF}$ = 7.4 Hz, $^4J_{HF}$ = 2.7 Hz, $^4J_{HF}$ = 1.0 Hz, 1F, CF). ^{31}P{^{1}H} NMR (CD_2Cl_2, 202.3 MHz, 21 °C): δ −40.67 (s, PMe$_3$).

[*exo*-Cp*Ir(PMe$_3$)(*anti*-η^3-$CH_2CHCFCF_2CF_3$)][B(ArF)$_4$] (7) and [*exo*-Cp*Ir(PMe$_3$)(*syn*-η^3-$CH_2CHCFCF_2CF_3$)][B(ArF)$_4$] (8). Cp*Ir-

(73) Pangborn, A. B.; Giardello, M. A.; Grubbs, R. H.; Rosen, R. K.; Timmers, F. J. *Organometallics* **1996**, *15*, 1518−1520.

(PMe_3)(*n*-C_3F_7)(CH═CH_2) (**5**) (9.5 mg, 0.0158 mmol) and lutidinium tetrakis(3,5-trifluoromethylphenyl)borate (15.4 mg, 0.0158 mmol) were placed in a J. Young's tube, and CD_2Cl_2 (0.7 mL) was added to dissolve the solids. At room temperature the reaction was complete within seconds. Compound **7** was formed along with compound **8** in a ratio ~6:1 and was identified by its NMR spectra.

^{1}H NMR (CD_2Cl_2, 500 MHz, 21 °C): δ 1.68 (dd, $^2J_{PH}$ = 10.3 Hz, $^4J_{FH}$ = 1.2 Hz, 9H, PMe_3), 1.93 (d, $^4J_{PH}$ = 1.9 Hz, 15H, Cp*), 2.54 (ddd, $^3J_{HH}$ = 10.0 Hz, $^2J_{HH}$ = 2.5 Hz, $^3J_{PH}$ = 16.5 Hz, 1H, syn-CH_2), 3.22 (ddd, $^3J_{HH}$ = 8.0 Hz, $^2J_{HH}$ = 2.5 Hz, $^3J_{PH}$ = 3.0 Hz, 1H, anti-CH_2), 4.40 (ddddd, $^3J_{HH}$ = 10.0 Hz, $^3J_{HH}$ = 8.0 Hz, $^3J_{FH}$ = 13.5 Hz, $^4J_{FH}$ = 5.0 Hz, $^3J_{PH}$ = 2.53 Hz, 1H, CH). ^{19}F NMR (CD_2Cl_2, 470.3 MHz, 21 °C): δ −82.59 (d, $^4J_{FF}$ = 14.3 Hz, 3F, CF_3), −111.88 (dd, $^2J_{F(AB)}$ = 274 Hz, $^3J_{FF}$ = 15.0 Hz, 1F, CF_2), −118.99 (dd, $^2J_{F(AB)}$ = 274 Hz, $^4J_{HF}$ = 5.0 Hz, 1F, CF_2), −153.97 (dqdd, $^3J_{FF}$ = 15.0 Hz, $^4J_{FF}$ = 14.3 Hz, $^3J_{HF}$ = 13.5 Hz, $^3J_{PF}$ = 7.5 Hz, 1F, CF). ^{31}P{^{1}H} NMR (CD_2Cl_2, 202.4 MHz, 21 °C): δ −48.30 (d, $^3J_{PF}$ = 7.5 Hz, 1P, PMe_3).

On standing for several hours at room temperature the resonances of **7** evolve into those of the thermodynamic product **8**. The solvent was removed in vacuo and the product extracted with ether. Removal of the ether afforded a pale yellow crystalline material, which was recrystallized from ether/hexanes to give X-ray quality crystals (22.8 mg, 99%).

Anal. Calcd for $C_{50}H_{39}BF_{30}IrP$: C, 41.59; H, 2.72. Found: C, 41.66; H, 2.84. ^{1}H NMR (CD_2Cl_2, 500 MHz, 21 °C): δ 1.59 (dd, $^2J_{PH}$ = 10.7 Hz, $^5J_{FH}$ = 1.3 Hz, 9H, PMe_3), 1.92 (dd, $^4J_{PH}$ = 1.8 Hz, $^5J_{FH}$ = 0.5 Hz, 15H, Cp*), 2.94 (ddddd, $^3J_{HH}$ = 10.0 Hz, $^2J_{HH}$ = 2.85 Hz, $^3J_{PH}$ = 13.6 Hz, $^5J_{FH}$ = 0.8 Hz, $^5J_{FH}$ = 0.8 Hz, 1H, syn-CH_2), 3.20 (ddddd, $^3J_{HH}$ = 7.4 Hz, $^2J_{HH}$ = 2.85 Hz, $^3J_{PH}$ = 0.9 Hz, $^4J_{FH}$ = 1.05 Hz, $^5J_{FH}$ = 1.8 Hz, 1H, anti-CH_2), 4.09 (dddddd, $^3J_{HH}$ = 10.0 Hz, $^3J_{HH}$ = 7.4 Hz, $^3J_{PH}$ = 1.9 Hz, $^3J_{FH}$ = 9.0 Hz, $^4J_{FH}$ = 2.25 Hz, $^4J_{FH}$ = 2.25 Hz, 1H, CH). ^{19}F NMR (CD_2Cl_2, 282.2 MHz, 21 °C): δ −82.41 (d, $^4J_{FF}$ = 13.6 Hz, 3F, CF_3), −115.43 (dd, $^2J_{F(AB)}$ = 282 Hz, $^3J_{FF}$ = 17.0 Hz, 1F, CF_2), −120.36 (dd, $^2J_{F(AB)}$ = 282 Hz, $^3J_{FF}$ = 7.5 Hz, 1F, CF_2), −181.79 (bd, $^3J_{PF}$ = 70.5 Hz, 1F, CF). ^{31}P{^{1}H} NMR (CD_2Cl_2, 121.4 MHz, 21 °C): δ −36.08 (d, $^3J_{PF}$ = 70.5 Hz, 1P, PMe_3).

***endo*-Cp*Ir(PMe_3)(*anti*-η^3-$CH_2CHCFCF_2CF_3$)[B(ArF)$_4$] (9).** Cp*Ir(PMe_3)(*n*-C_3F_7)(CH═CH_2) (9.5 mg, 0.158 mmol) was dissolved in CD_2Cl_2 (0.5 mL), and the resultant solution was placed in a J. Young's tube and stoppered with a septum. The tube was cooled in an acetone/dry ice bath, and a solution of lutidinium tetrakis(3,5-trifluoromethylphenyl)borate (15.4 mg, 0.0158 mmol) in CD_2Cl_2 (0.3 mL) was added dropwise by the side of the tube. The two layers were mixed while the sides of the tube were cooled by liquid nitrogen to avoid warming the sample. The tube was transferred to the NMR probe, which had been precooled to −50 °C. The product was observed by NMR spectroscopy at temperatures below −30 °C.

^{1}H NMR (CD_2Cl_2, 500 MHz, −50 °C): δ 1.52 (d, $^2J_{PH}$ = 10.7 Hz, 9H, PMe_3), 1.91 (d, $^4J_{PH}$ = 1.8 Hz, 15H, Cp*), 3.25 (bd, $^3J_{HH}$ = 12.0 Hz, 1H, syn-CH_2), 4.00 (dd, $^3J_{HH}$ = 7.9 Hz, $^2J_{HH}$ = 3.9 Hz, 1H, anti-CH_2), 4.72 (m, 1H, CH). ^{19}F NMR (CD_2Cl_2, 470.3 MHz, −50 °C): δ −80.66 (d, $^4J_{FF}$ = 12.2 Hz, 3F, CF_3), −112.89 (dd, $^2J_{F(AB)}$ = 279 Hz, $^3J_{FF}$ = 17.4 Hz, 1F, CF_2), −120.75 (d, $^2J_{F(AB)}$ = 279 Hz, 1F, CF_2), −158.23 (bs, 1F, CF). ^{31}P{^{1}H} NMR (CD_2Cl_2, 202.4 MHz, −50 °C): δ −37.88 (d, $^3J_{PF}$ = 21.3 Hz, 1P, PMe_3).

X-ray Crystal Structure Determinations. Diffraction intensity data were collected at 100 K with a Bruker Smart Apex CCD diffractometer. The structures were solved using the Patterson function, completed by subsequent difference Fourier syntheses, and refined by full matrix least-squares procedures on F^2. SADABS absorption corrections were applied (T_{min}/T_{max} = 0.706). Non-hydrogen atoms were refined with anisotropic displacement coefficients except the F atoms in disordered CF_3 groups, which were refined with isotropic thermal parameters. The hydrogen atoms were treated as idealized contributions. It was found that in the crystal structure of **8** the Ir atom, $CH_2CCFCF_2CF_3$, and PMe_3 groups in the cation are disordered in a ratio 74/26 over two positions approximately related by a mirror plane. Two CF_3 groups in the anion are disordered as well. All software and sources of scattering factors are contained in the SHELXTL (5.10) program package (G. Sheldrick, Bruker XRD, Madison, WI).

Acknowledgment. R.P.H. is grateful to the National Science Foundation for generous financial support of this research.

Supporting Information Available: Crystallographic information files (CIF) for compounds **5**, **6**, and **8**. This material is available free of charge via the Internet at http://pubs.acs.org.

JA042345D